

Kyle W. Hollman, C. M. Fortunko, Dale W. Fitting

National Institute of Standards and Technology
Materials Reliability Division
325 Broadway, Boulder, CO 80303

Abstract -- The objectives of this study are to determine the through-thickness elastic coefficient of fiber-epoxy/metal laminates with ultrasonic measurements and to determine the elastic coefficients of the constituent layers. For the measurements, a broadband, piezopolymer, transmitting transducer is excited with the leading edge of a square wave. A specimen is aligned perpendicular to the transducer in an immersion tank. Signals reflected from the specimen are captured by the piezopolymer transducer and Fourier transformed. Signals transmitted through the specimen are captured by a hydrophone, and the first arrival of the signals is used to determine the average velocity through the laminate. For this study we consider four regimes. There is a static regime and a second regime where the wavelength of the ultrasound is much greater than the thickness of the laminate. In the third, intermediate wavelength regime the velocities and densities of the individual layers are determined using "stop bands" in the spectrum. Short-duration pulse determinations of the elastic stiffness coefficients are valid in the forth, short wavelength regime. Elastic coefficients determined from pulse measurements compare favorably with predictions based on the assumption that velocities of the layers act in series as the sound travels through the laminate.

INTRODUCTION

The objective of this study was to provide insight into the development of a quantitative nondestructive method for testing the condition of fiber-epoxy/metal laminates. In working toward this goal, we sought to use ultrasonic measurements to determine the through-thickness elastic coefficient of the laminate and to determine the elastic coefficients of their constituent layers.

In evaluating the results of the ultrasonic measurements, we need to consider four regimes of interest: a static regime, a second regime where the wavelength of the ultrasound is greater than the thickness of the specimen, a third regime where the wavelength is of the same order of magnitude as the thickness, and a fourth regime where the wavelength is much shorter than the thickness. Our experiments are relevant to the intermediate- and short- wavelength regimes.

Shown in Figure 1, the specimen [1] used in our study consists of alternating layers of aluminum (2024 T3) and fiber-epoxy composites, all of which were 200 to 300 μm thick. The

fiber-epoxy layers consist of a unidirectional layup of aramid fibers in a polymer matrix. The two outer layers of the laminate are aluminum.

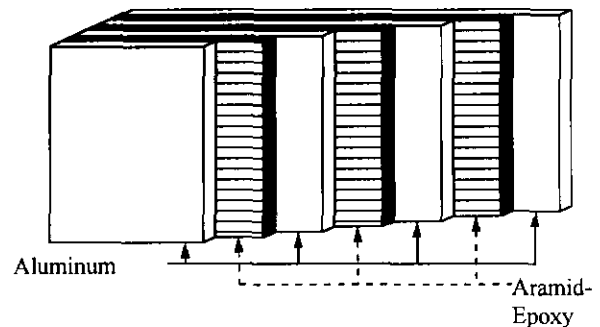


Figure 1. The layup of a typical fiber-epoxy/metal laminate

The laminate specimen is insonified in the experimental setup shown in Figure 2. Signals originate from a square wave generator and are amplified with an amplifier of low output impedance ($2\ \mu\Omega$) to produce a high-voltage (400 V) amplitude. After passing through a diplexer ("transmit-receive" switch) the signals excite a broadband (20 MHz) piezopolymer transmitting transducer. Signals reflected from a specimen aligned perpendicular to the transmitting transducer are captured by this same transducer. After passing through the diplexer, the back-reflected signals are amplified by a broadband receiver and displayed on a digital oscilloscope. These signals are transferred via a general-purpose interface bus (GPIB) to a personal computer for off-line analysis. Signals transmitted through the specimen are captured with a hydrophone (1 mm in diameter) and preamplifier. The transmitted signals are separately amplified by the receiver, displayed on the oscilloscope, and transferred to the computer for analysis.

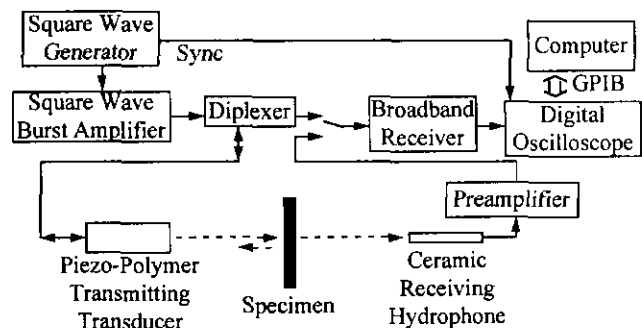


Figure 2. The block diagram of the experimental setup used for all measurements in this study

*Contribution of NIST. Not subject to copyright in the United States

Figure 3 shows the 20 μs long square wave that excites the piezopolymer transducer. As this figure indicates, both the rising and falling edges of the square wave create short-duration pulses. We capture 20 μs of the signals produced by the rising edge of the square wave as indicated by the dashed frame in the figure, avoiding those signals produced by the falling edge. The signal is captured on an 8-bit digitizer at a sampling rate of 100 MHz. The entire captured signal is Fourier transformed and displayed as an amplitude spectrum [2, 3].

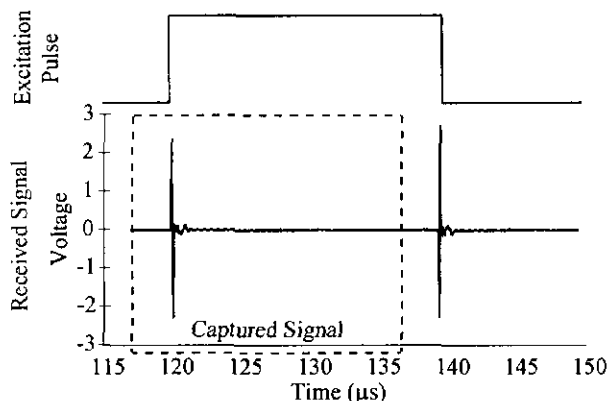


Figure 3. Square wave that excites the transmitting transducer and the resulting signal captured by the receiving transducer

The Fourier transform of a signal reflected from a specimen with 4 aluminum layers and 3 aramid-epoxy layers is shown in Figure 4. The general shape of this spectrum results mostly from the frequency response of the measurement system and the attenuation within the specimen. On top of this general shape, resonances appear as "stop bands" grouped into three distinct clusters. These resonances occur in a regime where the wavelength of the ultrasound is the same order of magnitude as the thickness of the specimen. The cluster of resonances near 10 MHz can be associated with the aluminum layers, the cluster near 6 MHz can be associated with the fiber-epoxy layers, and the cluster near 2 MHz can be associated with properties of the composite.

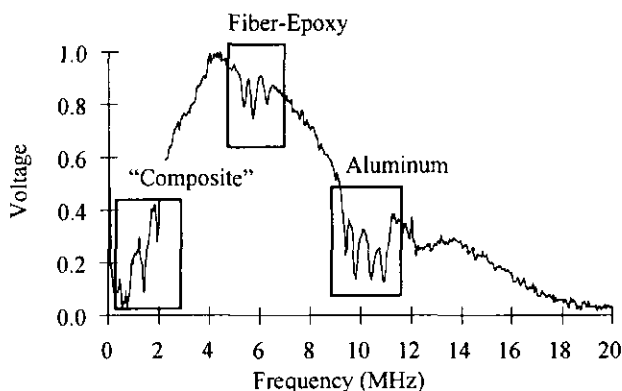


Figure 4. Spectrum of signals reflected from an aramid-epoxy/aluminum specimen

THEORY

The resonances in the spectrum and their behavior can be predicted with a theory developed by Folds and Loggins [4-7].

This theory was developed by matching the boundary conditions between each pair of layers in order to predict the reflection and transmission coefficients from materials with a finite number of layers. (This differs from Floquet theory, which was developed for materials with an infinite number of layers [7, 8].) In our use of this theory we calculate the reflection coefficient for a specimen aligned perpendicular to the transmitting transducer and ignore attenuation within the specimen.

Figure 5 demonstrates how the reflection coefficient calculated from the theory by Folds and Loggins changes as the configuration of aluminum and fiber-epoxy layers is changed. As the number of fiber-epoxy layers increases from 1 in the top panel to 2 in the middle panel to 3 in the bottom panel, there is a corresponding increase in the number of resonances in the highlighted cluster centered near 6 MHz. The same correspondence can be seen between the number of aluminum layers and the number of resonances in the highlighted cluster centered near 10 MHz. The resonances greater than 12 MHz are higher-order multiples of the cluster center at 6 MHz.

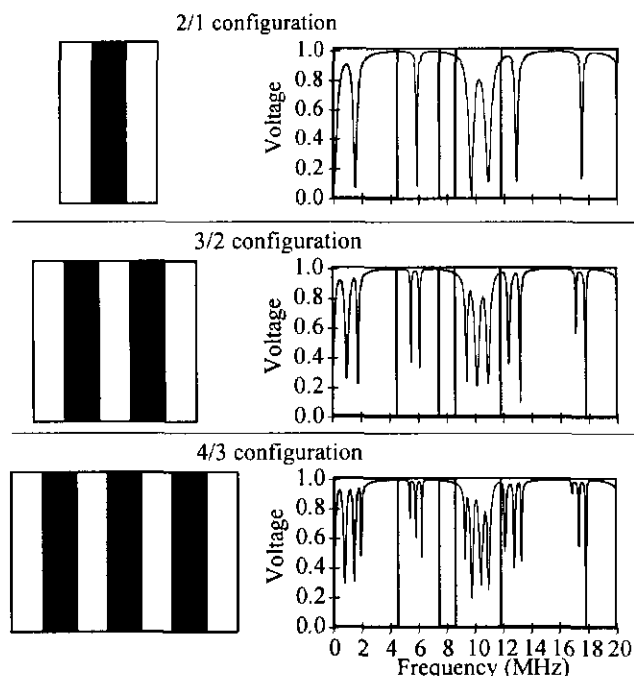


Figure 5. Reflection coefficient calculated from theory for three configurations of aluminum and fiber-epoxy layers

DATA ANALYSIS

The calculations from the theory developed by Folds and Loggins can be used to estimate the properties of the individual layers using a three-step process. First, the thicknesses of the layers are determined from optical micrographs. Next, the velocities in the theory are adjusted until the centroids of the clusters in the theory match the centroids of the clusters in the experimental data. Finally, the densities of the layers in the theory are adjusted until the fine details within each cluster match. Because the group velocity is indeterminate at the resonances, the velocities determined from this process must be phase velocities.

Using theoretical calculations, Figure 6 illustrates how steps 2 and 3 of the matching procedure function. The top panel of this figure shows how a 2% decrease in the velocity of the aramid-epoxy layer will shift all three resonances in this cluster towards a lower frequency, as indicated by the arrows. Increasing the velocity will shift them towards a higher frequency. The bottom panel indicates how the fine details within each cluster are matched by adjusting the density. In this panel the density of the aramid-epoxy layer is decreased by 10%, which results in a decrease in the interval between the resonances, as indicated by the arrows. An increase in the density will result in an increase in the interval. Changes in the properties of the aluminum layers will affect similar changes in the resonance locations of the aluminum cluster.

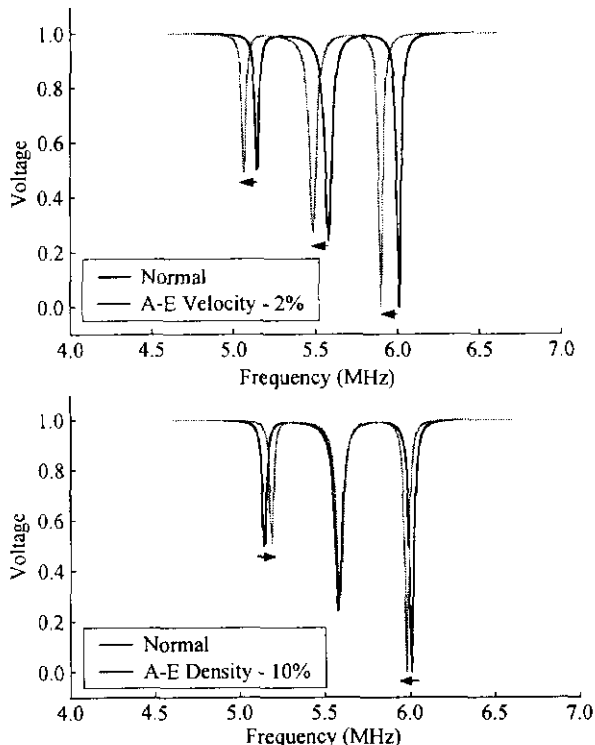


Figure 6. Changes in the location of the resonances caused by changes in the properties of the aramid-epoxy (A-E) layers

The changes made in Figure 6 are gross changes to illustrate the matching procedure. Our results show greater precision than the figure because we have the ability to zoom in to see more subtle changes. Changes in the properties of the aramid-epoxy affect mainly the aramid-epoxy cluster, and changes in the properties of the aluminum affect mainly the aluminum cluster; however these changes also have small influences on each other's cluster.

The result of matching the theory to the experimental data is shown in Figure 7. We do not do an exact fit of theory to experimental data [9]; rather we match the frequency locations of the resonances. As this figure indicates, the matching procedure worked quite well for this specimen.

The results of matching the theory to the experimental data for the aramid-epoxy/aluminum specimen are listed in Table I. The error indicated in this table represents the resolution of the reso-

nance matching procedure. This error is determined mostly by the frequency spacing of the spectrum, which in turn is determined by the sampling rate of the digitizer and the record length of the captured trace. Random noise can also influence this error.

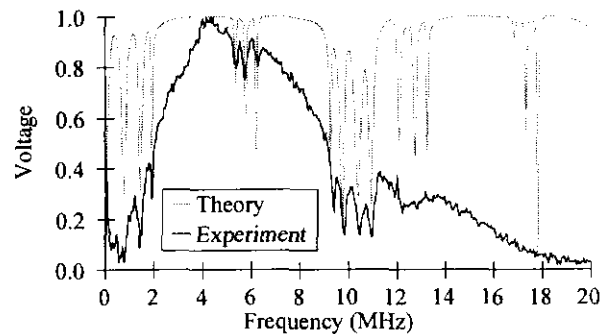


Figure 7. Theoretical match to the experimental data for signals reflected from a 4/3 configuration of aramid-epoxy/aluminum laminate.

Table I. Properties of the individual layers from matching theory to experimental data.

	Velocity (mm/ μ s)	Density (g/cm ³)
Aluminum	6.34 \pm 0.03	2.74 \pm 0.03
Aramid-Epoxy	2.51 \pm 0.01	1.36 \pm 0.01

SHORT-WAVELENGTH VELOCITY

The short-wavelength, through-thickness velocity of the specimen was determined from transmission measurements of the time of arrival of a short pulse using a piezopolymer transmitting transducer and a hydrophone receiving transducer (as shown in the block diagram in Figure 2). Timing was measured from the first arrival of the pulse. To obtain a velocity, two timing measurements are needed: the time t_0 the signal travels through the water path with the specimen removed, and the time t_1 through the water and the specimen. The average composite velocity v is determined by

$$v = \frac{d}{t_1 - t_0 + d / v_w}, \quad (1)$$

where d is the thickness of the composite and v_w is the velocity in water. The result of this measurement is listed in Table II.

Table II. Average laminate velocity (mm/ μ s)

Experiment (short wavelength)	4.026 \pm 0.129
Prediction (velocities in series)	4.133

The predicted velocity in Table II was computed using the assumption that the velocities of the layers act in series as the sound propagates through the laminate. The velocities of the layers as listed in Table I were used in the computation. The average predicted velocity of the composite compares well with the experimental, short-wavelength velocity, which is a more direct measure because it does not assume any relationship between the properties of the individual layers and the laminate.

Using a standard definition of the through-thickness elastic stiffness coefficient (the product of density and the square of the velocity) the average elastic stiffness coefficient of the laminate

can be calculated from Equation (2). If K is the elastic stiffness coefficient and n denotes the identity of the layer,

$$K = \frac{\sum_n \rho_n d_n}{\sum_n d_n} \left(\frac{\sum_n d_n}{\sum_n \frac{d_n}{v_n}} \right)^2, \quad (2)$$

where ρ is the density, d is the thickness, and v is the velocity. The first term in this equation represents the average density of the laminate and the second term represents the square of the laminate velocity.

This formulation of the elastic stiffness coefficient can be compared with the Reuss [10] and Voigt [11] formulations of the rule of mixtures. The average elastic stiffness coefficient K_R from the Reuss formulation is

$$K_R = \frac{\sum_n d_n}{\sum_n \frac{d_n}{\rho_n v_n^2}}, \quad (3)$$

and the average elastic stiffness coefficient K_V from the Voigt formulation is

$$K_V = \frac{\sum_n (\rho_n v_n^2) d_n}{\sum_n d_n}. \quad (4)$$

The difference between the three formulations is best exemplified by the summation of the velocities. In the velocity in series formulation, Equation (2), we calculate the square of the sum of the reciprocals of the velocities. This is similar to but contrasted with the Reuss formulation, Equation (3), which represents the elastic stiffness coefficients acting in series. In this formulation the squaring function is brought inside the summation. In the Voigt formulation, Equation (4), the elastic stiffness coefficients act in parallel and the summation of the square of the velocities occurs in the numerator.

We also compare our determinations with a formulation of combining the elastic stiffness coefficients proposed by Mori and Tanaka [12]. This method is based on averaging the internal stress in the matrix and considering the average elastic energy.

The Reuss and Voigt formulations represent the bounds for the rule of mixtures. As Table III shows, both our experimental determination as well as our prediction based on the velocities acting in series lie within these bounds, although they are closer to the Reuss bound. Table III also indicates that the experiment and prediction are in satisfactory agreement.

Table III. Elastic coefficients for aramid-epoxy/aluminum (GPa)

Experiment	36.6 ± 2.8
Prediction	38.5
Bounds for the Rule of Mixtures	
Voigt	74.5
Mori-Tanaka	21.3
Reuss	21.3

CONCLUSIONS

In evaluating the results of this study, we need to consider four regimes of interest. Mechanical testing is usually done in the static regime. Ultrasonic theory and testing are often done in

the regime where the wavelength of the sound is much greater than the thickness of the specimen. Our measurements using the back-reflected signal and our analysis of this signal using clusters of resonances in the spectrum are done in the intermediate wavelength regime. In this regime the wavelength is of the same order of magnitude as the thickness. The novel, three-step, resonance-matching procedure we present in this study produces precise determinations of the velocities and densities of the individual layers for fiber-epoxy/metal laminates.

The average velocity and elastic stiffness coefficient were determined in the short wavelength regime. The measured elastic stiffness coefficient fell within the accepted bounds of the rule of mixtures and compared favorably with a prediction based on the assumption that the velocities of the individual layers act in series as the wave propagates through the laminate.

ACKNOWLEDGMENTS

This work was partially supported by a National Research Council (NRC)/National Institute of Standards and Technology (NIST) postdoctoral research associateship. We thank C. N. McCowan for the optical micrography and the thickness measurements. We also thank W. Grandia of QMI Inc. for supplying the specimens and for his useful insights.

REFERENCES

- [1] H.F. Wu, L.L. Wu, and W.J. Slagter, "An investigation on the bearing test procedure for fibre-reinforced aluminum laminates," *J. Mater. Sci.*, vol. 29, pp. 4592-4603, 1994.
- [2] T. Pialucha, C.C.H. Guyott, and P. Cawley, "Amplitude spectrum method for the measurement of phase velocity," *Ultrasonics*, vol. 27, pp. 270-279, 1989.
- [3] T.M. Modderman, "Influence of the frequency behavior of ARALL and GLARE on the ultrasonic c-scan inspection," in *Review of Progress in QNDE*, 1995, pp. 1283-1290.
- [4] D.L. Folds and C.D. Loggins, "Transmission and reflection of ultrasonic waves in layered media," *J. Acoust. Soc. Am.*, vol. 62, pp. 1102-1109, 1977.
- [5] P.D. Jackins and G.C. Gaunard, "Resonance acoustic scattering from stacks of bonded elastic plates," *J. Acoust. Soc. Am.*, vol. 80, pp. 1762-1776, 1986.
- [6] L.M. Brekhovskikh, *Waves in Layered Media Second ed*, New York, NY: Academic Press, 1980, pp. 23-26.
- [7] A. Safaeinili and D.E. Chimenti, "Floquet analysis of guided waves in periodically layered composites," *J. Acoust. Soc. Am.*, vol. 98, pp. 2336-2342, 1995.
- [8] P.J. Shull, D.E. Chimenti, and S.K. Datta, "Elastic guided waves and the Floquet concept in periodically layered plates," *J. Acoust. Soc. Am.*, vol. 95, pp. 99-108, 1994.
- [9] V.K. Kinra, P.T. Jaminet, C. Zhu, and V.R. Iyer, "Simultaneous measurement of the acoustical properties of a thin-layered medium: The inverse problem," *J. Acoust. Soc. Am.*, vol. 95, pp. 3059-3074, 1994.
- [10] A. Reuss, "Berechnung der Fließgrenze von Mischkristallen auf Grund der Plastizitätsbedingung für Einkristalle," *Zeitschrift für Angewandte Mathematik und Physik*, vol. 9, pp. 49-58, 1929.
- [11] W. Voigt, *Lehrbuch der Kristallphysik*. Leipzig, Germany: Teubner, 1928.
- [12] T. Mori and K. Tanaka, "Average stress in matrix and average elastic energy of materials with misfitting inclusions," *Acta Metallurgica*, vol. 21, pp. 571-574, 1973.